

Field-induced anisotropic magnetization in the $\text{Ni}_{74}\text{Mn}_{24}\text{Pt}_2$ amorphous thin film

This article has been downloaded from IOPscience. Please scroll down to see the full text article.

1997 J. Phys.: Condens. Matter 9 6689

(<http://iopscience.iop.org/0953-8984/9/31/020>)

View [the table of contents for this issue](#), or go to the [journal homepage](#) for more

Download details:

IP Address: 171.66.16.207

The article was downloaded on 14/05/2010 at 09:18

Please note that [terms and conditions apply](#).

Field-induced anisotropic magnetization in the $\text{Ni}_{74}\text{Mn}_{24}\text{Pt}_2$ amorphous thin film

Y Öner†, A Kılıç‡ and S Senoussi§

† Department of Physics, Istanbul Technical University, 80626, Maslak, Istanbul, Turkey

‡ Department of Physics, Karaelmas University, Zonguldak, Turkey

§ Laboratoire de Physique des Solides (associé au CNRS, URA 0002), Université de Paris-Sud, 91405 Orsay Cédex, France

Received 20 December 1996, in final form 26 February 1997

Abstract. Magnetization measurements have been carried out on the $\text{Ni}_{74}\text{Mn}_{24}\text{Pt}_2$ amorphous thin film in magnetic fields up to 60 kG and in the temperature range 3–175 K for both the zero-field-cooling (ZFC) and field-cooling (FC) cases. At the lowest temperatures, for the FC case, the magnetization M parallel to the cooling field significantly differs from M perpendicular to it. This anisotropy was about 10 at $T = 3$ K and $H = 60$ kG, and it disappears completely at about $T = 10$ K. These results suggest cluster formation of strongly correlated and localized electrons. This assertion has been supported by resistivity measurements.

1. Introduction

NiMn alloys exhibit interesting magnetic properties due to the competition between the ferromagnetic exchange coupling of Ni–Ni or Ni–Mn pairs and the antiferromagnetic coupling of Mn–Mn pairs [1, 2]. In our recent studies [3, 4] and other similar work [5], it has been shown that the magnetic states and the electrical properties are significantly changed, especially at low temperatures, by the addition of a few atomic per cent of non-magnetic Pt impurities to Ni–Mn. More recently, we found [6] that the Pt impurities cause much more severe spin frustrations in the amorphous phase of this system compared to that in the corresponding polycrystalline phase. Thus, one might well ask what the interplay is between disordered (including both structural and magnetic) and electron interactions, in governing the electronic and magnetic properties of this amorphous system. Our present study will contribute experimentally to the work based on this fundamental question in condensed matter, to which a rich variety of theoretical approaches have been developed over the last decade [7–9].

Here, we present magnetization measurements for the $\text{Ni}_{74}\text{Mn}_{24}\text{Pt}_2$ amorphous thin film in the 3–175 K temperature range. An anisotropy observed at $H = 60$ kG—the magnetization along the cooling field direction compared to that perpendicular to it—was larger than 10. These results suggest cluster formation of strongly correlated and localized electrons in the amorphous $\text{Ni}_{74}\text{Mn}_{24}\text{Pt}_2$ alloy. The resistivity in the field $H = 120$ kG increases drastically with decreasing temperature after passing through a minimum at about $T \sim 30$ K. This behaviour has been attributed to cluster formation of electrons [10].

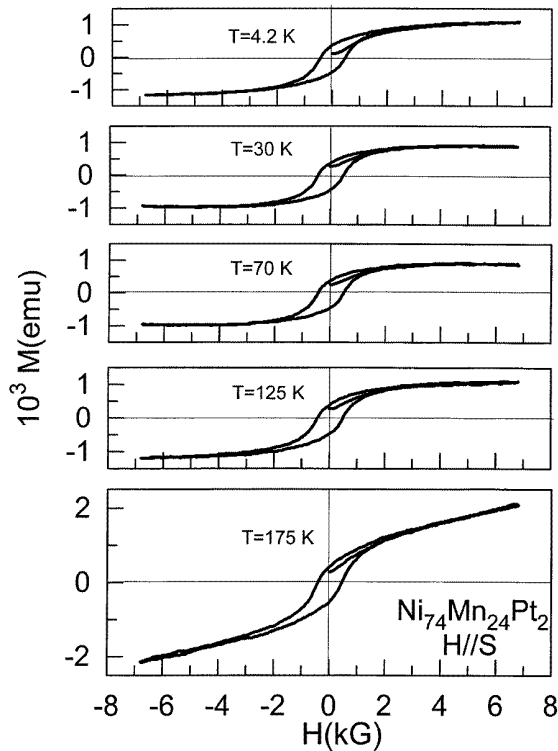


Figure 1. Magnetization hysteresis loops for parallel geometry (the measuring field parallel to the film surface) at the temperatures indicated in the figure. The film was first cooled from room temperature to 4.2 K in zero field, and then the temperature was increased step by step while the magnetization versus the measuring field between -7 kG and $+7$ kG was recorded at each temperature. Note that the magnetization at higher temperatures does not saturate at 7 kG.

2. Experimental results

The amorphous $\text{Ni}_{74}\text{Mn}_{24}\text{Pt}_2$ film alloys were prepared by using the flash evaporation technique. The details of this technique have been described elsewhere [11]. The thickness of these films is about 2000 \AA .

The hysteresis cycles were achieved by means of a vibrating-sample magnetometer (VSM) whose sensitivity is about 10^{-5} emu. The magnetic field was produced by a 70 kG superconducting magnet. The temperature was controlled by a carbon-glass and platinum resistance located near the sample.

The resistivity measurements were performed by using the AC technique. The voltage accuracy was better than one part in 10^7 . The magnetic field (0–160 kG) was supplied using a superconducting magnet. The temperature was monitored and controlled via a carbon-glass thermometer to within an estimated accuracy of 0.01 K below 40 K and 0.05 K above 100 K.

The magnetization data were obtained under the four different sets of conditions, described below.

(i) The film was first cooled to 4.2 K for parallel geometry in zero field (the ZFC case for parallel geometry). The magnetization of this film was measured while the applied field

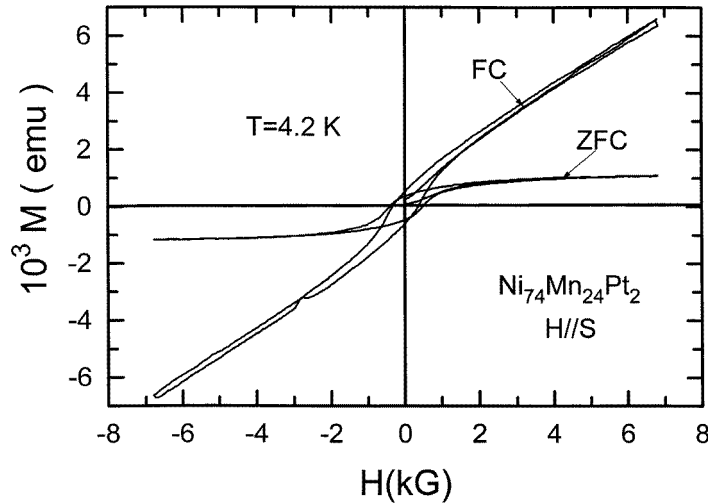


Figure 2. Magnetization hysteresis loops for parallel geometry at $T = 4.2$ K. Note that FC and ZFC indicate the cases in which the film was cooled in the applied field of 7 kG, parallel to the film surface, from $T = 175$ K to $T = 4.2$ K (just after plotting the hysteresis loop at $T = 175$ K for the ZFC case) and the case in which it was cooled in zero field, respectively. It is of interest to note that the magnetization for the FC case does not saturate, and it is much larger than that for the ZFC case.

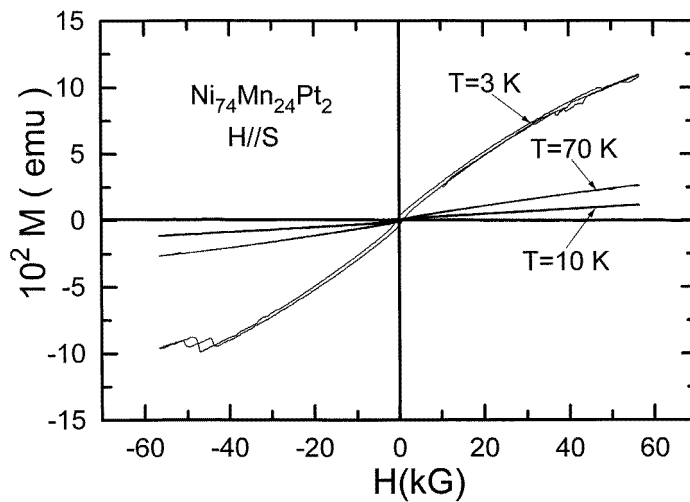


Figure 3. Magnetization hysteresis loops between -60 kG and $+60$ kG for parallel geometry at $T = 3$ K, 10 K, and 70 K, with the presence of the induced anisotropic magnetization. Note that this anisotropy almost disappears at $T = 10$ K.

was slowly cycled between ± 7 kG; thus, we always obtained a complete hysteresis. We continued these measurements at higher temperatures up to $T = 175$ K. Figure 1 shows the M versus H hysteresis cycles for some selected temperatures for the ZFC case.

(ii) After reaching $T = 175$ K, the film was then allowed to cool back to the lowest temperature ($T \sim 3$ K) while retaining the field of 7 kG, parallel to the film surface,

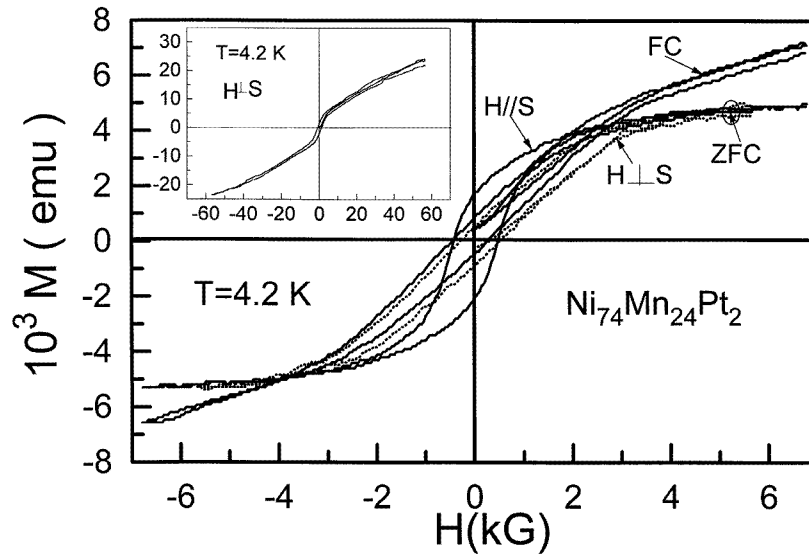


Figure 4. Magnetization hysteresis loops for both parallel and perpendicular geometries at $T = 4.2$ K. The film was cooled from $T = 175$ K to $T = 4.2$ K in zero field and in a field of 7 kG applied parallel to the measuring field direction and in the same field when it was applied perpendicularly. Since the hysteresis for the ZFC case and that for the case in which the cooling field is perpendicular to the measuring field are almost the same, the hysteresis loop for the latter case is not shown. The inset shows the hysteresis loop for the perpendicular geometry between -60 kG and $+60$ kG for the FC case.

and, subsequently, the M versus H hysteresis cycle was recorded between ± 60 kG. Then, the film was slowly warmed up to higher temperatures in steps of about 10 K, and the hysteresis loops were recorded at each temperature. This situation is called the parallel-field-cooled case (\parallel FC), meaning that the cooling field is parallel to the measuring field. Figure 2 displays the hysteresis loops at $T = 4.2$ K for the ZFC case and the \parallel FC case between ± 7 kG. Figure 3 shows the hysteresis cycles at three different temperatures. It is obvious from these figures that the hystereses for the \parallel FC case at the lowest temperatures, below $T = 6$ K, considerably differ from those for the ZFC case in some respects. The magnetization does not saturate even at $H = 60$ kG. Particularly striking is the fact that the reversible component of the magnetization is significantly enhanced (by a factor of 10 at $H = 60$ kG) compared to those for the ZFC case. However, this enhancement in the magnetization disappears at temperatures above $T = 10$ K.

(iii) In the following step, the sample was cooled down to 4.2 K in a field of 7 kG parallel to the film surface, and then was taken out of the set-up. After rotating the sample by 90° from its initial position, the sample was reinserted inside the sample zone in zero field for temperatures down to $T = 4.2$ K, and the hysteresis loops were recorded. This situation is called the perpendicular-field-cooled case (\perp FC), meaning that the cooling field is perpendicular to the measuring field. Obviously, the new loop exhibits the same behaviour as that of the ZFC case for perpendicular geometry; the magnetization first increases linearly due to the demagnetizing field, and then levels off at a certain value of the applied field.

(iv) Finally, the film was rotated again to its initial position outside of the set-up ($T = 300$ K), and then it was cooled down to $T = 3$ K in zero field. Surprisingly, we observed that the recorded loop at $T = 3$ K for this case was almost the same as that for

the \parallel FC case; i.e. the anisotropy in the magnetization was still persisting. After annealing the film outside of the set-up ($T = 300$ K) for at least two days, we found that the film had completely lost the enhanced magnetization. We also repeated the same experiment for the case in which the applied field was initially perpendicular to the film surface (see figure 4). The induced magnetization was first created along the direction perpendicular to the film surface (see the inset to figure 4). We have observed similar behaviours for this experiment. It can be seen that there is no major difference among the loops for both parallel and perpendicular geometries, except as regards the level of the enhancement of the magnetization. We recognized that, during many similar experiments carried out on different films with the same composition, this enhancement depends a little on the thermal and magnetic history of the film and the cooling field.

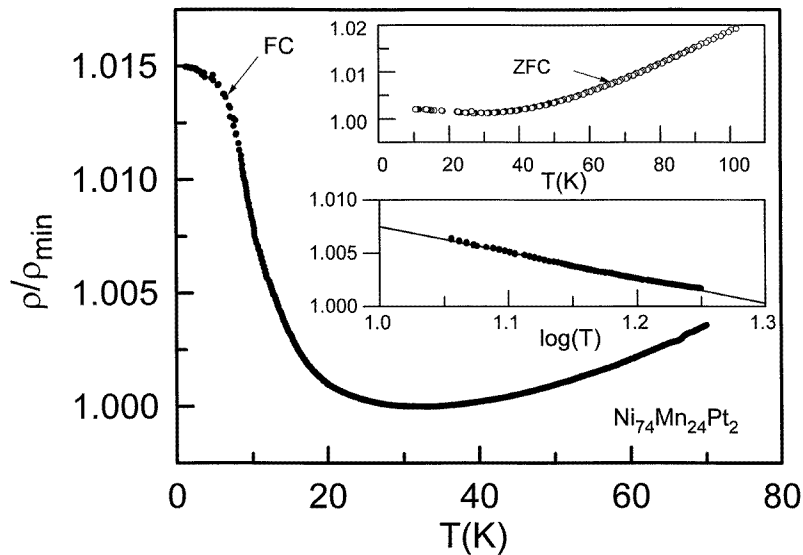


Figure 5. Low-temperature resistivity data on the amorphous $Ni_{74}Mn_{24}Pt_2$ thin film. The upper inset shows the resistivity versus temperature for the zero-field-cooling (ZFC) case. The lower inset represents the logarithmic temperature dependence of the normalized resistivity $\rho(T)/\rho_{min}$ for the ZFC case at temperatures below T_{min} (the temperature of the minimum in $\rho(T)$). Note that the normalized resistivity $\rho(T)/\rho_{min}$ for the FC case increases drastically at temperatures below T_{min} compared to that for the ZFC case (they differ by a factor of 5). Here the cooling field was 120 kG.

The resistivity measurements were performed for two different sets of conditions.

(i) First, the resistivity of the film was measured as a function of the temperature while it was allowed to cool slowly down to $T = 1.5$ K from $T \sim 150$ K in zero magnetic field (see the inset to figure 5). As seen in the inset to figure 5, the resistivity exhibits a resistivity minimum at about $T = 30$ K. The depth of the resistivity minimum $(\rho(1.6 \text{ K}) - \rho_{min})/\rho(1.6 \text{ K})$ is about 3×10^{-3} . The other inset represents a semi-logarithmic plot of the resistivity associated with this sample for the zero-field-cooling case. A detailed discussion of the temperature behaviour of the resistivity was given in reference [12].

(ii) Secondly, the film was warmed up to about $T = 200$ K, and then was allowed to cool down to the lowest temperature in the magnetic field $H = 120$ kG, while the resistivity was recorded. As seen in figure 5, the resistivity passes through a minimum at

about $T = 30$ K, and then increases drastically at lower temperatures. The depth of the resistivity minimum described above for this case is 1.5×10^{-2} , which is five times greater than that for the zero-field case. It should be noted that the low-temperature resistivity data for the field-cooling case do not follow a logarithmic behaviour; the resistivity levels off at the lowest temperatures.

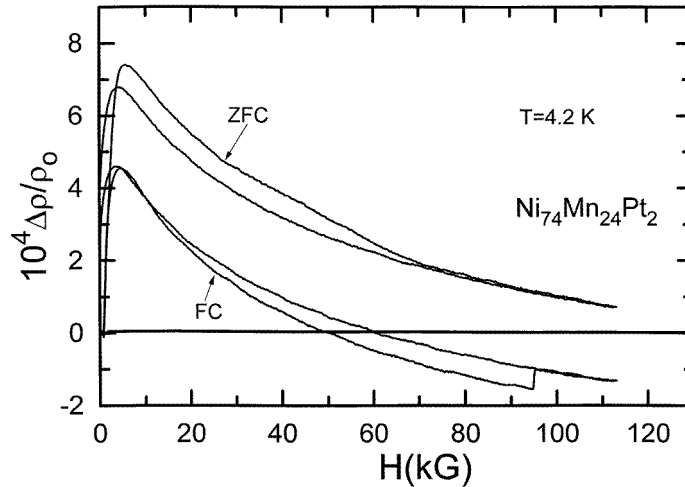


Figure 6. The field dependence of the magnetoresistance of the $\text{Ni}_{74}\text{Mn}_{24}\text{Pt}_2$ thin film at $T = 4.2$ K for both the zero-field-cooling (ZFC) and field-cooling (FC) cases.

We have also carried out magnetoresistance measurements at $T = 4.2$ K on this film for both the zero-field-cooling and field-cooling cases. The results are given in figure 6. It is clear from the figure that the magnetoresistance $\Delta\rho/\rho_0$ varies approximately as H^2 at lower fields, and then evolves towards a linear variation as a function of H at higher fields for both cases. This kind of behaviour has often been observed for the archetypical spin glasses AuFe and CuMn. Therefore, the low-temperature behaviour of $\Delta\rho/\rho_0$ seems to be suggestive of a spin-glass-like (or related) order. The difference between the curves for the zero-field-cooling and field-cooling cases can be attributed to the thermoremanent alignment. It is well known that, if the demagnetized state is non-ideal, the zero of the magnetoresistance will be shifted up or down, but the total magnetoresistance $\Delta\rho_t/\rho$, resulting from a change from one saturated state (with the magnetic field parallel to both the film surface and the measuring current) to another (with the magnetic field perpendicular to the film surface), will remain the same.

3. Discussion

From our very recent ESR study [6] performed on the same film, we know that this film exhibits a very strong spin disorder at a microscopic scale at low temperatures. This causes the resonance spectra to broaden with decreasing temperature, so they could not be analysed. More recently, our electrical measurements [12] have demonstrated that the disorder-enhanced interactions are important in determining the temperature dependence of the conductivity at the lowest temperatures (it displays a resistivity minimum). On the other hand, the most ideal spin-glass behaviour without a displaced hysteresis loop for the

amorphous phase of NiMn was also reported by Hauser and Bernardini [13]. It appears that the localization of electrons in this amorphous structure plays a major role as regards the anisotropy observed in the magnetization. This is probably caused by the strongly interacting electron gas in such a disordered matrix. Fortunately, as David G Rowan and co-workers [9] have pointed out, spatial disorder leads to a strong site-differential enhancement of the local susceptibilities. They found that the local susceptibility for the strong-local-moment sites is well over an order of magnitude larger than the Pauli susceptibility for the corresponding non-interacting electron gas. From the above considerations, we believe that the interactions between electrons are so strong that electrons start to form a cluster around some sites. The sudden increase in the reversible component of the magnetization at low temperatures may be attributed to cluster formation of the electrons.

In order to give added support to the above conclusions, we also give the resistivity data taken on the same film under the same conditions as those for the magnetization measurements. Taking the magnetoresistivity effect at $H = 120$ kG (which is of the order of 10^{-4}) into account, one may suggest that such an increment in the resistivity at temperatures well below the temperature of the resistivity minimum could be due to the decrease in the mobilities of the conduction electrons. In other words, the electrons strongly correlate with each other, resulting in a decrease of the conductivity. The behaviour of the resistivity seems to be consistent with the magnetization data. The model based on cluster formation of the electrons appears to give a good account of the behaviour of both the magnetization and the resistivity at low temperatures. This is not to say, however, that this picture can explain all of the behaviour observed for this film. On the basis of the present data, it appears that the formation of the clusters occurs only along the axis of the cooling field. However, further study is needed to confirm this observation. A sceptical reader may propose an alternative explanation for these results; but in view of its successes we wish to retain it.

Acknowledgments

This work was supported by NATO Grant No CRG 940539 and by The Scientific and Technical Research Council of Turkey (TUBITAK) through Project No TBAG-1365.

References

- [1] Kouvel J S 1961 *J. Phys. Chem. Solids* **21** 57
- [2] Kouvel J S, Abdul-Razzaq W and Ziq Kh 1987 *Phys. Rev. B* **35** 1768 and references therein
- [3] Öner Y and Aktaş B 1990 *Phys. Rev. B* **42** 2425
- [4] Durusoy Z H and Öner Y 1990 *Phys. Rev. B* **42** 6831
Aktaş B, Öner Y and Harris E A 1989 *Phys. Rev. B* **39** 528
- [5] Ando T, Ohta E and Sato T 1997 *J. Magn. Magn. Mater.* **163** 277
- [6] Öner Y, Özdemir M, Aktaş B, Topaçlı C, Harris E A and Senoussi S 1997 *J. Magn. Magn. Mater.* at press
- [7] Lee P A and Ramakrishnan T V 1985 *Rev. Mod. Phys.* **57** 287
- [8] Belitz D and Kirkpatrick T R 1994 *Rev. Mod. Phys.* **66** 261
- [9] Rowan D G, Szczech Y H, Tusch M A and Logan D E 1995 *J. Phys.: Condens. Matter* **7** 6853
- [10] Finlayson D M (ed) 1986 *Localization and Interaction in Disordered Metals and Doped Semiconductors* (*Scottish Universities Summer School in Physics 31*) (Bristol: Institute of Physics Publishing) p 195
- [11] Kiliç A, Öner Y and Çelik H 1995 *J. Magn. Magn. Mater.* **146** 298
- [12] Öner Y, Kiliç A and Çelik H 1995 *Physica B* **215** 205
- [13] Hauser J S and Bernardini J E 1984 *Phys. Rev. B* **30** 3803